Provided for non-commercial research and education use.
Not for reproduction, distribution or commercial use.

This article appeared in a journal published by Elsevier. The attached copy is furnished to the author for internal non-commercial research and education use, including for instruction at the authors institution and sharing with colleagues.

Other uses, including reproduction and distribution, or selling or licensing copies, or posting to personal, institutional or third party websites are prohibited.

In most cases authors are permitted to post their version of the article (e.g. in Word or Tex form) to their personal website or institutional repository. Authors requiring further information regarding Elsevier's archiving and manuscript policies are encouraged to visit:

http://www.elsevier.com/copyright

Author's personal copy

Available online at www.sciencedirect.com
ScienceDirect
Current Opinion in Microbiology

Physical principles and models describing intracellular virus particle dynamics☆

T Lagache, E Dauty and D Holcman

Modeling in cellular biology benefits greatly from quantitative analysis that arise from the theory of diffusion and chemical reactions. Recent progress in single particle imaging enables the visualization of viral trajectories evolving in the cytoplasm. Biophysical models and mathematical analysis have been developed to unravel the complexity of single viral trajectories. We review here models of active motion of viruses along the cytoskeleton as well as their diffusion. We present resent efforts to estimate global trafficking properties, such as the probability and the mean time for a viral particle to reach a small nuclear pore. However, most signaling pathways involved in controlling viral motion remain undescribed and should be the goal of future modeling efforts.

Address
Department of Biology and Mathematics, Ecole Normale Supérieure, 46 rue d'Ulm, 75005 Paris, France

Corresponding author: Holcman, D (holcman@biologie.ens.fr)
☆This research is supported by an ERC-starting grant.

Current Opinion in Microbiology 2009, **12**:439–445

This review comes from a themed issue on
Host–microbe interactions: viruses
Edited by Lucas Pelkmans

Available online 14th July 2009

1369-5274/$ – see front matter
© 2009 Elsevier Ltd. All rights reserved.

DOI 10.1016/j.mib.2009.06.015

Introduction

Animal viruses which replicate in the nucleus invade mammalian cells through a multistep process, often starting with endocytosis. Following this step, viral particles have to escape from the hostile environment of the endosomal lumen and move through the cell cytoplasm before reaching the nucleus. In this review, we discuss recent modeling efforts made to describe viral trajectory at a single unit level. Elucidating viral motion is essential in developing quantitative models and simulations. When combined to imaging, they allow to reveal unexpected aspects of intracellular trafficking [1••]. Understanding the cytoplasmic viral journey shall also serve to improve and optimize virus-based gene delivery vectors.

Single material particle trajectories were first described by Newton' second law of motion, which accounts for the field of forces. The trajectory is completely determined by the initial conditions and is obtained by solving a second order differential equation, integrating twice the acceleration to the position. In contrast, the motion of a particle constantly perturbed by random collisions is not any more predictable, but still, as recognized by Langevin, such trajectories can be analyzed by introducing stochastic terms in Newton's equation. In a medium at equilibrium, these stochastic terms are known explicitly [2] and are related to the average thermodynamically quantities (the temperature) or fluid properties (the friction coefficient). Furthermore, in an overdamped medium (a fluid), the acceleration term in the Langevin equation can be dropped and we are left with a stochastic equation for the velocity [2]. To analyze viral particle trajectories, we start from microscopic interactions and use a stochastic description. We also discuss the endosomal transport and present estimates for the probability and the mean time of infection. Such models integrate both passive transport (Brownian motion) and active transport (motion along microtubules (MTs) and actin filaments) (Figure 1).

Describing viral trajectories in the cytoplasm

Because viruses have no means of locomotion, they entirely rely on diffusion and cellular transport systems to reach the cellular compartments where they multiply. The cell cytoplasm is a highly crowded fluid containing many organelles, a cytoskeleton and diffusible macromolecules of high concentration [3]. The mobility depends on many parameters such as the size, the shape, and the nature of the interactions between viral particle and the surrounding cellular components. Noninteracting spherical particles with size up to $\approx 25\,\text{nm}$ are freely diffusible in the cell cytoplasm [4]. Increasing the size above 45 nm reduces the motion considerably.

The early mathematical models [5–7] to quantify the success of genome delivery are based on mass-action law to account for the transition from different cellular compartments (entering inside the cell, escaping from vesicles, nuclear entry) and the possible degradation. These approaches present several limitations: they are valid only at a population level and cannot be generalized to describe single particles. They do not account for the cellular geometry and rely specifically on rate constants that are usually unknown and thus fitted to data rather than derived from biophysical analysis. In [8], an alternative approach using the cellular geometry,

Author's personal copy

Figure 1

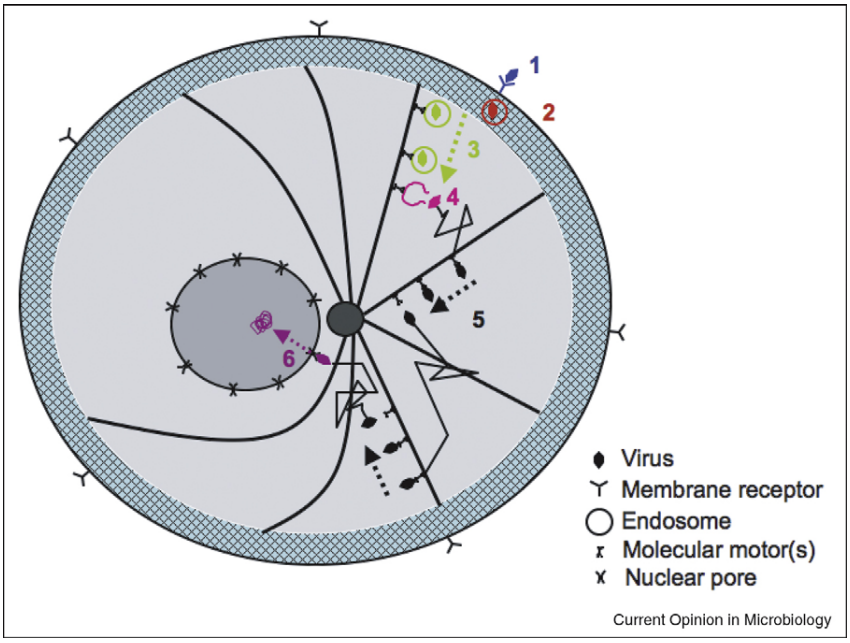

(1) A viral particle binds to a specific receptor and is internalized in an endosome. (2) Virus traffics inside the endosome through the cortical actin network. (3) The virus is transported actively in the endosome along the MTs. (4) Virus escapes from the endosome. (5) The viral motion alternates between diffusion and active transport along the MTs. (6) Virus finally reaches a nuclear pore and delivers its genetic material.

allowed the authors to give a macroscopic description of the adenovirus concentration so that they can analyze the effect of varying the number of MTs on the invasion process. Using a new reconstruction imaging technique, this group has extended their analysis to polymer-based vectors [9•].

Recent progress using single particle tracking has revealed the complexity of viral trajectories [10,11,12•]. It has now been recognized that such trajectories consist of a succession of free or confined diffusion and/or ballistic periods. These later involve transport along MTs or actin networks which requires energy. Although diffusion in various media is well understood, it is not clear how active transport involves molecular motors [13]. The precise description of viral trajectories requires modeling the field of forces applied on single particles. In general, the analysis of random trajectories of particles is formulated in terms of stochastic equations. The position at time t of a particle is treated as a stochastic process [2,14] and the dynamics depends on the forces applied on the particle.

In the cytoplasm, the high frequency collisions between a viral particle and the rest of the molecules are modeled by the classical noise term $\sqrt{2D}(d\mathbf{W}/dt)$, where D is the diffusion constant and W is the white noise (random variable with a Gaussian distribution of mean 0 and variance 1). In the absence of any other forces, the equation for the velocity is $(d\mathbf{X}/dt) = \sqrt{2D}\,(d\mathbf{W}/dt)$ and the trajectory is the standard Brownian motion. When diffusion and active transport occur simultaneously, the equation for the velocity becomes $(d\mathbf{X}/dt) = \mathbf{b}(\mathbf{X}) + \sqrt{2D}\,(d\mathbf{W}/dt)$, where $\mathbf{b}$ is the drift. Such description allows to generate computer simulations of trajectories [2,15] in free and confined environment [16] and is the basis to derive formula for the total probability of reaching a particular target [17•]. When an unshaped particle switches between diffusion and an active transport, the physical description of the position $X(t)$ at time t is

$$\dot{\mathbf{X}} = \begin{cases} \sqrt{2D}\dot{\mathbf{w}} & \text{for a free particle,} \\ \mathbf{V}(s(t)) & \text{for a bound particle,} \end{cases} \quad (1)$$

where the variable $s(t)$ describes the internal state, accounting for the nature and the number of bound motors going to the plus or minus MT ends. $\mathbf{V}$ is the resulting transport field defined by the MTs network organization, and it depends on the load exerted by the transported virus on motors. When the field $\mathbf{V}(s(t))$ is determined by the velocity amplitude $V_{i,j}$ associated with i bound kinesins and j dyneins, the transition dynamics between the different states is defined by the rates $k_{i,j}$ between states and the dissociation rate $k^d_{i,j}$ from (i,j) to a pure Brownian dynamics. The association rate from pure Brownian to a binding state depends in

Author's personal copy

particular on the geometrical organization of the MTs and the cell [18,19•]. It would be interesting to analyze how the host–virus interactions define the switching rates $k_{i,j}, k^d_{i,j}$ and the velocities $V_{i,j}$. Indeed, many viruses such as herpes virus [20], adenovirus [21] or HIV [22] bind motors of different polarities which lead to a bidirectional transport. A regulatory mechanism should favor the switch dynamics in one direction leading to a net velocity in that particular direction [23]. While traveling in one direction, it is not clear whether dyneins or kinesins work cooperatively [24•], which should influence the resulting velocity [24•,25]. An enveloped virus can be seen as a fluid like cargo, while motors should rigidly bind to naked viruses [26].

Although the previous description using Eq. (1) may allow to generate simulations of trajectories, we cannot use it for a general analysis. However, through a mathematical procedure [18,19•], the switching dynamics (1) can be coarsely grained so that the velocity $\dot{\mathbf{X}}$ can be written as the sum of an permanent effective drift term $\mathbf{b}(\mathbf{X})$ that accounts for the ballistic periods along the MTs and the random interactions noise term $\sqrt{2D}(d\mathbf{W}/dt)$

$$\frac{d\mathbf{X}}{dt} = \mathbf{b}(\mathbf{X}) + \sqrt{2D}\,\frac{d\mathbf{W}}{dt}, \tag{2}$$

where the effective velocity $\mathbf{b}(\mathbf{X})$ depends on the forward and backward binding rates and the mean net velocity $\bar{\mathbf{V}}$ along MTs, obtained by averaging $\mathbf{V}$ over the time. A calibration procedure to obtain such an expression is described in [19•]. Interestingly, the backward rate of cargos from the MT decreases with the number of bound motors [25,27,28]. We will explain later how this average description is used to derive analytical formulas that combine all input parameters, characterizing the infection success. We shall recall that using computer simulations, we can only explore a small fraction of the parameter space, but on the contrary a full analytical expression provides the total dependency and is usually a great help to characterize various regimes. Analytical expressions are usually very difficult to obtain, but when some parameters are much smaller than others, asymptotic formulas can be derived which relate all the parameters together.

Confined motion

Besides diffusion and directed transport along cytoskeleton, restricted and confined motion can appear in various conditions. Confined dynamics have been studied both experimentally and theoretically [29–32]. The simplest case is the physical restriction by impenetrable barriers. When the barrier represents a large portion of a three-dimensional domain, the time to escape such region is given $\tau \approx Vol/4Da$, where Vol is the volume, D the diffusion constant and a is the size of the small opening disk [17•]. Direct chemical interactions by a local potential can also generate a confined motion, in that case the time to escape is the reciprocal of the activation rate [2] and depends exponentially on the interaction potential. A third possibility occurs when a cargo or a virus binds simultaneously motors that travel in opposite directions: the stochastic switch between directions lead to a confined trajectory over a characteristic distance, that depends on the exchange rate. This situation has been described as a 'tug of war' [33,34]. In brief, confined motions resulting from either physical reflection on obstacles or direct chemical reactions, are the consequences of the viral dynamics in the complex cytoplasmic environment and can be characterized by the mean time to escape confinement [17•,29,31].

From the local cytoplasm trafficking properties to the probability and the mean time to arrive at a small nuclear pore

The probability and the mean time to reach a nuclear pore provide a global quantification of the cytoplasmic viral infection step. Such quantities depend on the local motion, the degradation rate, the MT organization and the geometry of the cell and can be estimated asymptotically [35,36] when the diffusion is smaller compared to the active motion. To derive such estimates, the rational is to start from the individual description Eq. (2). We will only browse here the general method and use references for the details. In that spirit, early physical considerations [37] led to a closed formula for the mean time τ a diffusing particle (with a diffusion coefficient D) moving in a confined domain of volume Vol, to hit one of n small patches of radius η located on a sphere of radius δ. It is given by [37]

$$\tau = Vol\left(\frac{1}{4\pi D\delta} + \frac{1-p_A}{4nD\eta}\right), \tag{3}$$

where $p_A = (n\pi\eta^2)/(4\pi\delta^2)$ is the ratio of n patches surface to the sphere area. Interestingly, we can obtain both quantitative and qualitative information from formula (3). Indeed, we learn that the surface covered by the patches is not determinant compared to the number of holes: it is more efficient to cover a sphere with many small holes of very small radius than to have a single big hole [36]. Actually, in the case of pure diffusion, many absorbing small holes are equivalent to an almost totally absorbing surface [38]. However, the description of a viral particle reaching a small target is a bit more complex due to the interactions with kinesins and dyneins. The number of motors, their binding regulation, and the resulting velocity [13] are determined in a complex manner by several factors. As described above, in a coarse grained description of viral trajectory, the complex motion involving motors and free motion can be reduced to an effective drift and a Brownian component (2).

Author's personal copy

Using classical statistical physics [2,15], we will now present how to link the single particle with the macroscopic description and other global measurable quantities. To describe the viral journey in the cytoplasm, we shall account for the viral degradation or immobilization, modeled by a steady state degradation rate $k(\mathbf{x})$. To describe the probability P_N, that a single virus arrives to a small nuclear pore alive and the associated mean time τ_N, we shall first introduce the survival probability density function (SPDF) $p(\boldsymbol{x},t)$. It is the probability to find the viral particle alive (not degraded) and inside a cytoplasmic volume element $\boldsymbol{x}+d\boldsymbol{x}$ at time t. It is defined by [35],

$$p(\boldsymbol{x},t)d\boldsymbol{x} = Pr\{X(t)\in \boldsymbol{x}+d\boldsymbol{x}, \quad \tau^k > t, \quad \tau^a > t | p_i\}, \quad (4)$$

where τ^a is the first time for a live virus to arrive to one of the nuclear pore areas, denoted ∂N_a, τ^k the first time that it is degraded, and p_i is the viral initial distribution. The important and deep result [2] is that the SPDF $p(x,t)$ satisfies a partial differential equation, known as the Fokker–Planck equation (FPE)

$$\begin{aligned} &\frac{\partial p}{\partial t}(\boldsymbol{x},t) = D\Delta p(\boldsymbol{x},t) - \nabla\cdot \boldsymbol{b}(\boldsymbol{x})p(\boldsymbol{x},t) - k(\boldsymbol{x})p(\boldsymbol{x},t) \quad \text{for} \quad \boldsymbol{x}\in\Omega,\\ &p(\boldsymbol{x},0) = p_i(\boldsymbol{x}) \quad \text{for} \quad \boldsymbol{x}\in\Omega, \end{aligned} \quad (5)$$

which describes how the probability to find a random particle evolves in time. The first term in the right-hand side is the contribution of the pure diffusion, the second term corresponds to the drift, and the last term is coming from the degradation and says that at each moment of time, the particle can potentially be destroyed. To account for the boundary effect, we add the conditions

$$\begin{aligned} &p(\boldsymbol{x},t) = 0 \quad \text{for} \quad \boldsymbol{x}\in\partial N_a,\\ &\boldsymbol{J}(\boldsymbol{x},t)\cdot\boldsymbol{n}_{\boldsymbol{x}} = 0 \quad \boldsymbol{x}\in\partial\Omega - \partial N_a, \end{aligned} \quad (6)$$

where the first condition says that the probability to find the particle on ∂N_a is zero. This is the part of the boundary where it is absorbed irreversibly. This condition is an idealized description of a nuclear pore where upon hitting this surface, the particle is instantaneously translocated to the nucleus with probability one and thus disappears from the cytoplasm. The second condition given on $\partial\Omega - \partial N_a$ is the remaining reflecting area of cell surface, describing a reflected particle, $\boldsymbol{n}_{\boldsymbol{x}}$ is the unit outer normal at a boundary point $\boldsymbol{x}$. This second condition is defined by the flux density vector $\boldsymbol{J}(\boldsymbol{x},t)$ as

$$\boldsymbol{J}(\boldsymbol{x},t) = -D\nabla p(\boldsymbol{x},t) + \boldsymbol{b}(\boldsymbol{x})p(\boldsymbol{x},t) \quad (7)$$

and is zero when no viral particle penetrates the membrane surface. The exciting property is that the probability P_N that a live virus arrives at the nucleus can be expressed using the SPDF. Indeed, it is the probability to arrive to a nuclear pore before being degraded and is thus total survival flux to the absorbing boundary

$$P_N = Pr\{\tau^a < \tau^k\} = \int_{\partial N_a}\int_0^\infty \boldsymbol{J}(\boldsymbol{x},t)\cdot\boldsymbol{n}_{\boldsymbol{x}} dS_{\boldsymbol{x}} dt \quad (8)$$

and the conditional mean time is given by

$$\begin{aligned} \tau_N &= [\tau^a \,|\, \tau^a < \tau^k] = \int_0^\infty (1 - Pr\{\tau^a < t \,|\, \tau^a < \tau^k\})\, dt\\ &= P_N \int_0^\infty \int_{\partial N_a} t\boldsymbol{J}(\boldsymbol{x},t)\cdot\boldsymbol{n}_{\boldsymbol{x}}\, dS_{\boldsymbol{x}}\, dt, \end{aligned} \quad (9)$$

where $Pr\{\tau^a < t | \tau^a < \tau^k\}$ is the probability density function of the time to absorption, conditioned on the event to arrive alive. Based on the small hole theory [17•], general asymptotic expressions of P_N and τ_N can be derived [35]. For simplicity, we shall present here the closed expressions obtained for flat cells (small thickness h) and when the diffusion is smaller than the directed motion time scale, there are [19•]:

$$\begin{aligned} P_N &= \frac{b(\delta)}{ln(1/\epsilon)2\delta k_0 + b(\delta)} \text{ and } \tau_N\\ &= \frac{ln(1/\epsilon)2\delta}{ln(1/\epsilon)2\delta k_0 + b(\delta)}, \end{aligned} \quad (10)$$

where δ is the radius of the nucleus, k_0 is the constant degradation rate near the nucleus, $b(\delta)$ is the drift amplitude given below (see Eq. (11)) and ϵ is the fraction of the nucleus covered by nuclear pores. b depends on the mean net velocity $\bar{V}$ on MTs, the viral unbinding rate k^{-1}, the MT network organization and other viral properties such as the cytoplasmic diffusion constant D and the effective viral diameter d. For N MTs, radially distributed, the drift is given by [19•]:

$$b(\delta) = \frac{\bar{V} - (\delta k^{-1}/12)(2\pi h/N(2\gamma+d))^2}{1 + (k\delta^2/12D)(2\pi h/N(2\gamma+d))^2}, \quad (11)$$

where γ is the interaction range between molecular motors and MTs [40]. Formula (10) says that most of the typical trajectories are destroyed near the nucleus and interestingly, the nucleus radius is a fundamental parameter, not the surface. We can use them to estimate the infection process. We have summarized in Table 1 the reported measured data for the adeno-associated virus (AAV) and in Table 2 we present our associated predictions for τ_N and P_N.

The present approach is quite general and for the particular case of AAV infection, our results predict that the

Author's personal copy

Table 1

Model parameters.

Parameters	Description	Value
δ	Nuclear radius	$\delta = 8\,\mu m$
ϵ	Nuclear pores relative surface	$\epsilon = 2\%$ [39]
N	Number of MTs	$N = 800$ [40]
h	Cell thickness	$h = 9\,\mu m$ [40]
k_0	Degradation rate (measured for plasmids)	$k_0 = 1/3600\,s^{-1}$ [41]
γ	Interaction range between motors and MTs	$\gamma = 50\,nm$[40]
D	Cytoplasmic diffusion of the virus	$D = 1.3\,\mu m^2\,s^{-1}$ (for the AAV [10])
d	Diameter of the virus	$d = 30\,nm$ (for the AAV [10])
$\bar{V}$	Averaged net velocity of the virus on MTs	$\bar{V} = 0.2\,\mu m\,s^{-1}$ (10% [42] of the minus end velocity $2\,\mu m\,s^{-1}$ [10])
k^{-1}	Virus unbinding rate from MTs	$k^{-1} = 0.05\,s^{-1}$ (dynein processivity [43])

Table 2

Prediction of the probability and mean time.

Model outputs	Description	Value
τ_N	Mean first passage time of a live virus to a nuclear pore	$\tau_N = 317\,s \approx 5\,min$
P_N	Probability a virus reaches a nuclear pore before being degraded	$P_N = 91\%$

efficiency is above 90%, while the mean time to reach a nuclear pore is around 5 min. This time accounts only for the free cytoplasmic journey. Since the time between virus entry and nuclear import was reported to be around 15 min [10], we suggest that the endosomal step should last about 10 min (which is the time needed by an early endosome to maturate into a late endosome [44]).

We end this section by pointing out the possible links between various physical parameters we have described here and the host–virus signaling. Indeed, either these parameters are directly measurable such as the diffusion constant, the degradation rate or the velocity along the MTs or they are computed (the mean velocity along the MTs, the association rate . . .). However, the host cell interaction can modify this set of parameters. Indeed, by controlling the level of tau-proteins, the cell regulates the binding rate of molecular motors to the MTs and thus the velocity of the transported viruses [45]. It would be interesting to measure the viral velocity along MTs for various concentrations of tau-proteins. Moreover, the MT organization can also be modified by viral infection, which is the case for the vacinia virus [46]. Indeed, vacinia viruses can interact with the rho family, which results in an increase in the dynamics of MTs. These effects can be taken into account by modifying the velocity field in our equations and thus will affect the probability and the time of infection.

Endosomal trafficking

Another fundamental aspect of viral trafficking concerns the sojourn in the endosomal compartment. A top-down approach to study how the endocytic membrane and protein kinases regulate the endocytic machinery is reviewed in [47]. To escape endosomes, before a critical time, the viral payload is usually assisted by glycoproteins for enveloped viruses or penetration proteins for naked viral particles. To fulfill their goal these proteins have to undergo a conformational change often resulting from endosome acidification. Because the exit time plays a critical role in the viral infectivity process, a recent model (T. Lagache *et al.*, unpublished) has been developed to estimate the escape time. Using a discreet Markov jump analysis [48,49], we first estimate, at a given pH, the mean time the number of bound protons (or other pH-activated ligands) reaches a critical threshold, which triggers the conformational change of a given glycoprotein or penetration protein. Combining these computations with experimental data [50] on the mean number of protons bound to HA1 (a subunit of the influenza hemagglutinin (HA)), we recovered measured conformational change kinetics [51] and confirmed the hypothesis that only HA1 conformational change is pH-dependent and other rearrangements in HA proceed spontaneously [50,52].

Combining the conformational change discreet model described above with an endosomal Poissonnian entry of ligands, we derived for viruses that contain a small number of glycoproteins or penetration proteins the mean escape time from the endosome and the associated pH. In the computations, we have considered that viruses escape from the endosome when at least one conformational change occurs. In particular, we found that for AAV the mean time to escape is around $20 \pm 5\,min$ (which is coherent with the observed 10 min) and when the virus has to escape in a pH range of 6.1–6.3, this is optimally achieved when five viral particles are inside an endosome. Finally, this biophysical model predicts that the size of the endosome, which may vary following endosomal fusion or split [44], does not impact the escape much.

Perspective: how future models should account for host–virus regulations

How virus trafficking involves the host–virus interaction remains unclear. However, such interactions may be controlled by the cell itself through regulatory mechanisms.

Author's personal copy

For example by controlling the level of tau-proteins, the cell regulates the binding rate of molecular motors to the MTs and thus the velocity of transported viruses [45]. In addition, by taking into account the host–virus interactions, it will allow us to further analyze how various parameters, such as the mean transport velocity, the binding and unbinding rates, the organization of MTs, the degradation rate, and many others are modified. This analysis should reveal the specificity of each viral infection and its relation to the cell response.

More specifically, concerning early steps of viral infection, we can identify three functional modules in which the host–virus interaction modulates the viral trajectory and the infection process. These modules interact with one another through a complex host-cell communication and they require specific biophysical modelings: first, during the entrance step, viruses interact with specific cell surface receptors, that will determine the fate and/or the viral pathway in the cytoplasm. For example, fusion proteins of widely disparate enveloped viruses completely metamorphose during viral entry [53]. In particular, the interaction of the retrovirus avian leukosis virus with the cell membrane specific receptor transforms its pH-independent glycoproteins to pH-dependent ones. As a consequence the fusogenic activity at low pH [54] is deployed which is necessary for the endosomal escape. In the case of AAV, cells and serotype specific receptors lead to a broad class of endocytic pathways [55]. Each pathway is characterized by a specific endosomal environment and an escape dynamical process, both lead to different viral escape location. In addition, the number of viruses per endosome should be crucial for the escape dynamics (T. Lagache *et al.*, unpublished). It will interesting to study for each cases the fraction of viral particles that can reach the nucleus. The second module consists of the endosomal step. Although, the escape time from endosomes can be computed from the conformational changes of viral active proteins (T. Lagache *et al.*, unpublished), the escape location depends on the surface receptor interactions (first module). Both the escape location and the associated pH are key input parameters for the third module, which consists of the free cytoplasmic step starting from the endosomal escape and ending at a nuclear pore. For example, the pH-dependent AAV capsid denaturation in the endosome should impact its cytoplasmic ubiquitination [56] that will in turn competitively increase its proteasome-mediated degradation and enhance capsid disassembly and subsequent nuclear import [56]. Although this degradation process can be accounted directly in the degradation rate k, a refined model would be needed to describe in detail how this competition process influences viral trajectories.

Finally, to find the optimal infection pathways, all three modules should be coupled and the output parameters of one will serve as the inputs for the next one. For example, in the case of AAV, it would be interesting to determine how the escape pH and subsequent capsid denaturation impacts cytoplasmic degradation rate k through the proteasome-mediated digestion of the capsid. Because each virus is routed to a specific pathway through a complex host-cell communication, a quantitative analysis of each single pathway would be needed. More fascinating, as viruses infect cells and the host cell interaction starts to change, viruses should see a different cell environment depending on their arrival time at the surface.

References and recommended reading

Papers of special interest, published within the period of review, have been highlighted as:

- • of special interest
- •• of outstanding interest

1. •• Damm EM, Pelkmans L: **Systems biology of virus entry in mammalian cells**. *Cell Microbiol* 2006, **8**:1219-1227.
Description of the host–virus interaction through molecular signaling.

2. Schuss Z: *Theory and Applications of Stochastic Differential Equations*. John Wiley & Sons Inc.; 1980.

3. Medalia O, Weber I, Frangakis AS, Nicastro D, Gerisch G, Baumeister W: **Macromolecular architecture in eukaryotic cells visualized by cryoelectron tomography**. *Science* 2002, **298**:1209-1213.

4. Seksek O, Biwersi J, Verkman AS: **Translational diffusion of macromolecule-sized solutes in cytoplasm and nucleus**. *J Cell Biol* 1997, **138**:131-142.

5. Dee K, Shuler ML: **Optimization of an assay for baculovirus titer and design of regimens for the synchronous infection of insect cells**. *Biotechnol Prog* 1997, **13**:14-24.

6. Varga CM, Hong K, Lauffenburger DA: **Quantitative analysis of synthetic gene delivery vector design properties**. *Mol Ther* 2001, **5**:438-446.

7. Banks GA, Roselli RJ, Chen R, Giorgio TD: **A model for the analysis of nonviral gene therapy**. *Gene Ther* 2003, **20**:1766-1775.

8. Dinh AT, Theofanous T, Mitragotri S: **A model for intracellular trafficking of adenoviral vectors**. *Biophys J* 2005, **89**:1574-1588.

9. • Dinh AT, Pangarkar C, Theofanous T, Mitragotri S: **Understanding intracellular transport processes pertinent to synthetic gene delivery via stochastic simulations and sensitivity analyses**. *Biophys J* 2007, **92**:831-846.
An extension to polymer-based vectors of their model developed to describe the intracellular trafficking of adenoviruses (Biophys J 89 (2005)). Interestingly, a new reconstruction imaging technique is used.

10. Seisenberger G, Ried MU, Endress T, BYning H, Hallek M, BrSuchle C: **Real-time single-molecule imaging of the infection pathway of an adeno-associated virus**. *Science* 2001, **294**:1929-1932.

11. Arhel N, Genovesio A, Kim KA, Miko S, Perret E, Olivo-Marin JC, Shorte S, Charneau P: **Quantitative four-dimensional tracking of cytoplasmic and nuclear HIV-1 complexes**. *Nat Methods* 2006, **10**:817-824.

12. • Brandenburg B, Zhuang X: **Virus trafficking — learning from single-virus tracking**. *Nat Rev Microbiol* 2007, **5**:197-208.
Very complete and comprehensive overview of new single-virus tracking techniques. It describes how these new imaging techniques help to monitor the journey that viruses make through cells and how it can be used to elucidate the entry, trafficking and egress mechanisms of various animal viruses.

13. Vale RD: **The molecular motor toolbox for intracellular transport**. *Cell* 2003, **112**:467-480.

14. Berg HC: *Random Walks in Biology*. Princeton University Press; 1983.

Author's personal copy

15. Risken H: *The Fokker–Planck Equation: Methods of Solutions and Applications*Springer; 1996.

16. Singer A, Schuss Z, Osipov A, Holcman D: **Partially reflected diffusion**. *SIAM J Appl Math* 2007, **68**:844-868.

17. • Schuss Z, Singer A, Holcman D: **The narrow escape problem for diffusion in cellular microdomains**. *Proc Natl Acad Sci U S A* 2007, **104**:16098-16103.
This paper gives new asymptotic estimates for the mean escape time of a Brownian diffusing particle confined to a bounded domain (a compartment or a cell) by a reflecting boundary, except for a small window through which it can escape.

18. Lagache T, Holcman D: **Effective motion of a virus trafficking inside a biological cell**. *SIAM J Appl Math* 2008, **68**:1146-1167.

19. • Lagache T, Holcman D: **Quantifying intermittent transport in cell cytoplasm**. *Phys Rev E Stat Nonlin Soft Matter Phys* 2008, **77**:030901.
This paper presents a general methodology to replace ballistic periods along MTs by an effective drift in a Langevin description of trajectories. It gives related estimates for the mean time and the probability a virus reaches a small nuclear pore.

20. Smith GA, Gross SP, Enquist LW: **Herpesviruses use bidirectional fast-axonal transport to spread in sensory neurons**. *Proc Natl Acad Sci U S A* 2001, **98**:3466-3470.

21. Suomalainen M, Nakano MY, Keller S, Boucke K, Stidwill RP, Greber UF: **MT-dependent plus- and minus end-directed motilities are competing processes for nuclear targeting of adenovirus**. *J Cell Biol* 1999, **144**:657-672.

22. McDonald D, Vodicka MA, Lucero G, Svitkina TM, Borisy GG, Emerman M, Hope TJ: **Visualization of the intracellular behavior of HIV in living cells**. *J Cell Biol* 2002, **159**:441-452.

23. Gross SP: **Hither and yon: a review of bi-directional MT-based transport**. *Phys Biol* 2004, **1**:1-11.

24. • Leduc C, Ruhnow F, Howard J, Diez S: **Detection of fractional steps in cargo movement by the collective operation of kinesin-1 motors**. *Proc Natl Acad Sci U S A* 2007, **104**:10847-10852.
By detecting fractional steps of kinesin-1 *in vitro*, this paper indicates a lack of synchronization between motors carrying a same cargo.

25. Klumpp S, Lipowsky R: **Cooperative cargo transport by several molecular motors**. *Proc Natl Acad Sci U S A* 2005, **102**:17284-17289.

26. Campàs O, Leduc C, Bassereau P, Casademunt J, Joanny JF, Prost J: **Coordination of kinesin motors pulling on fluid membranes**. *Biophys J* 2008, **94**:5009-5017.

27. Howard J, Hudspeth AJ, Vale RD: **Movement of MTs by single kinesin molecules**. *Nature* 1989, **342**:154-158.

28. Block SM, Goldstein LS, Schnapp BJ: **Bead movement by single kinesin molecules studied with optical tweezers**. *Nature* 1990, **348**:348-352.

29. Saxton MJ: **Single-particle tracking: effects of corrals**. *Biophys J* 1995, **69**:389-398.

30. Saxton MJ: **Lateral diffusion in an archipelago. Single-particle diffusion**. *Biophys J* 1993, **64**:1766-1780.

31. Kusumi A, Sako Y, Yamamoto M: **Confined lateral diffusion of membrane receptors as studied by single particle tracking (nanovid microscopy). Effects of calcium-induced differentiation in cultured epithelial cells**. *Biophys J* 1993, **65**:2021-2040.

32. Salman H, Abu-Arish A, Oliel S, Loyter A, Klafter J, Granek R, Elbaum M: **Nuclear localization signal peptides induce molecular delivery along MTs**. *Biophys J* 2005, **89**:2134-2145.

33. Valleriani A, Liepelt S, Lipowsky R: **Dwell time distributions for kinesin's mechanical steps**. *EPL* 2008, **82**:28011.

34. Gross SP, Welte MA, Block SM, Wieschaus EF: **Coordination of opposite-polarity MT motors**. *J Cell Biol* 2002, **156**:715-724.

35. Holcman D: **Modeling viral and DNA trafficking in the cytoplasm of a cell**. *J Stat Phys* 2007, **127**:471-494.

36. Lagache T, Dauty E, Holcman D: **Quantitative analysis of virus and plasmid trafficking in cells**. *Phys Rev E Stat Nonlin Soft Matter Phys* 2009, **79**:011921.

37. Zwanzig R: **Diffusion-controlled ligand binding to spheres partially covered by receptors: an effective medium treatment**. *Proc Natl Acad Sci U S A* 1990, **87**:5856-5857.

38. Berg HC, Purcell EM: **Physics of chemoreception**. *Biophys J* 1977, **20**:193-219.

39. Maul GG, Deaven L: **Quantitative determination of nuclear pore complexes in cycling cells with differing DNA content**. *J Cell Biol* 1977, **73**:748-760.

40. Ndlec F, Surrey T, Maggs AC: **Dynamic concentration of motors in MT arrays**. *Phys Rev Lett* 2001, **86**:3192-3195.

41. Lechardeur D, Sohn KJ, Haardt M, Joshi PB, Monck M, Graham RW, Beatty B, Squire J, O'Brodovich H, Lukacs GL: **Metabolic instability of plasmid DNA in the cytosol: a potential barrier to gene transfer**. *Gene Ther* 1999, **6**:482-497.

42. Suomalainen M, Nakano MY, Keller S, Boucke K, Stidwill RP, Greber UF: **MT-dependent plus- and minus end-directed motilities are competing processes for nuclear targeting of adenovirus**. *J Cell Biol* 1999, **144**:657-672.

43. Reck-Peterson SL, Yildiz A, Carter AP, Gennerich A, Zhang N, Vale RD: **Single-molecule analysis of dynein processivity and stepping behavior**. *Cell* 2006, **126**:335-348.

44. Rink J, Ghigo E, Kalaidzidis Y, Zerial M: **Rab conversion as a mechanism of progression from early to late endosomes**. *Cell* 2005, **122**:735-749.

45. Vershinin M, Carter BC, Razafsky DS, King SJ, Gross SP: **Multiple-motor based transport and its regulation by Tau**. *Proc Natl Acad Sci U S A* 2007, **104**:87-92.

46. Valderrama F, Cordeiro JV, Schleich S, Frischknecht F, Way M: **Vaccinia virus-induced cell motility requires F11L-mediated inhibition of RhoA signaling**. *Science* 2006, **311**:377-381.

47. Liberali P, Rämö P, Pelkmans L: **Protein kinases: starting a molecular systems view of endocytosis**. *Annu Rev Cell Dev Biol* 2008, **24**:501-523.

48. Knessl C, Mangel M, Matkowsky BJ, Schuss Z, Tier C: **Solution of Kramers–Moyal equations for problems in chemical physics**. *J Chem Phys* 1984, **81**:1285-1293.

49. Matkowsky BJ, Schuss Z, Knessl C, Tier C, Mangel M: **Asymptotic solution of the Kramers–Moyal equation and first passage times for Markov jump processes**. *Phys Rev A* 1984, **29**:3359-3369.

50. Huang Q, Opitz R, Knapp EW, Herrmann A: **Protonation and stability of the globular domain of influenza virus hemagglutinin**. *Biophys J* 2002, **82**:1050-1058.

51. Krumbiegel M, Herrmann A, Blumenthal R: **Kinetics of the low pH-induced conformational changes and fusogenic activity of influenza hemagglutinin**. *Biophys J* 1994, **67**:2355-2360.

52. Huang Q, Korte T, Rachakonda PS, Knapp EW, Herrmann A: **Energetics of the loop-to-helix transition leading to the coiled-coil structure of influenza virus hemagglutinin HA2 subunits**. *Proteins* 2009, **74**:291-303.

53. Dutch RE, Jardetzky TS, Lamb RA: **Virus membrane fusion proteins: biological machines that undergo a metamorphosis**. *Biosci Rep* 2000, **20**:597-612.

54. Mothes W, Boerger AL, Narayan S, Cunningham JM, Young JA: **Retroviral entry mediated by receptor priming and low pH triggering of an envelope glycoprotein**. *Cell* 2000, **103**:679-689.

55. Ding W, Zhang L, Yan Z, Engelhardt JF: **Intracellular trafficking of adeno-associated viral vectors**. *Gene Ther* 2005, **12**:873-880.

56. Yan Z, Zak R, Luxton GW, Ritchie TC, Bantel-Schaal U, Engelhardt JF: **Ubiquitination of both adeno-associated virus type 2 and 5 capsid proteins affects the transduction efficiency of recombinant vectors**. *J Virol* 2002, **76**:2043-2053.